Power Dispatch Estimation from Electric Vehicles in a Distribution System

Ganesh K. Venayagamoorthy, *Fellow, IEEE*
Real-Time Power and Intelligent Systems Laboratory, Holcombe Department of Electrical and Computer Engineering
Clemson University, Clemson, SC, USA
Department of Electrical, Electronic and Computer Engineering, University of Pretoria, South Africa
gkumar@ieee.org

Imanthi Kalanika Subasinghe, *Graduate Student Member, IEEE*
Real-Time Power and Intelligent Systems Laboratory
Holcombe Department of Electrical and Computer Engineering
Clemson University, Clemson, SC, USA
imanthi@ieee.org

Raj Naidoo, *Senior Member, IEEE*
Department of Electrical, Electronic and Computer Engineering
University of Pretoria, South Africa
raj.naidoo@up.ac.za

2024 7th International Conference on Electric Power and Energy Conversion Systems (EPECS) | 979-8-3315-1696-3/24/$31.00 ©2024 IEEE | DOI: 10.1109/EPECS62845.2024.10805530

***Abstract*—The integration of electric vehicles (EVs) into the electric power distribution system poses numerous challenges and opportunities for optimizing energy management and system operations. Electric vehicle grid interfaces (EVGIs), essentially bidirectional power converters, allow for charging/grid-to-vehicle (G2V) and discharging/vehicle-to-grid (V2G) power transfers. A power dispatch estimation (PDE) model for V2G, based on availability of EVs in a distribution system and capabilities of the distribution system, is needed to assist in grid operations. This paper presents the development of a PDE model based on nodal power flows to capture the complex spatiotemporal dependencies inherent in G2V and V2G patterns. The hierarchical structure of a distribution system, feeder to EVGI node, is taken into consideration for PDE. Typical PDE estimation results are presented for the IEEE 34 test node feeder distribution system allocated with EVGIs.**

Keywords— Distribution system, electric vehicles, estimation, G2V, power dispatch, V2G.

I. Introduction

In the drive towards achieving carbon neutrality by 2050, the global energy sector is witnessing a significant surge in the adoption of electric vehicles (EVs) [1]. This transition is pivotal in aligning with the goal of limiting the global temperature rise to 1.5°C, as advocated by the Intergovernmental Panel on Climate Change. This upward trajectory is expected to continue [2]. More recently, the emergence of smart grid concept and the advancement of Vehicle-to-Grid (V2G) technology has reshaped the role of EVs [3]. V2G facilitates bidirectional energy exchange between EVs and the power grid [4], offering a spectrum of services aimed at enhancing grid reliability and efficiency [5, 6]. These services include regulation, spinning reserve, peak load management, load balancing and reactive power compensation. Given the intricacies with V2G power dispatch, which entails a multifaceted unit commitment problem with competing objectives and constraints, optimization techniques become indispensable [7].

Power dispatch from the EVs to the grid involves determining the optimal allocation of available generation resources to meet the demand at any given time. Knowing the potential V2G discharge brings situational intelligence to grid operators to be able to allocate resources optimally and efficiently, reducing the need for expensive peaking power plants and making better use of renewable energy sources. Accurate power dispatch estimation (PDE) assist in maintaining the balance between electricity generation and demand, which is essential for stability, security and reliability of the power grid. Unpredicted surges or sudden reductions in demand can cause voltage fluctuations, frequency instability, and even blackouts. V2G enables demand response management where EVs can be charged during off-peak periods and discharge during peak periods, effectively shifting loads and flattening the demand curve [7, 8].

Plug-in hybrid EVs, battery EVs and fuel cell EVs poses the capability to establish a connection with the grid, enabling bidirectional power flow for both charging (G2V) and discharging (V2G). This V2G functionality holds the potential as mentioned above to enhance grid efficiency and reliability significantly, especially with renewable energy [9]. Understanding the statistical availability of vehicles for charging or discharging is essential [4]. In the contemporary distribution grid, distributed generation units, often relying on intermittent renewable energy resources (RESs), have become more prevalent. In [4], the integrated approach optimally aligns consumption and generation, enhancing overall energy efficiency and grid stability.

Another application for leveraging EVs is for energy storage in order to maximize the utilization of photovoltaic energy [5], initially intended for propulsion. Integrating EVs into the grid alongside RESs offers a range of benefits. A model for an EV storage system within a standardized power system, specifically utilizing the IEEE 30-node power system model was presented in [6]. A decision-making strategy was formulated to guide the deployment of stored battery energy, considering factors such as the state of charge, time of day, electricity prices, and the charging requirements of an EV.

This paper presents an estimation model for V2G power dispatch based nodal EV discharging across a distribution system, leveraging its capabilities. The hierarchical architecture of a distribution system is three layered as follows: EVGI level, nodal level and feeder level, respectively, shown in Fig. 1. Furthermore, Monte Carlo simulation is used to estimate the number of available EVs to carry out V2G dispatch. The modified IEEE 34 test node feeder, representing a real distribution system in Arizona, is utilized for the illustrating the PDE model proposed in this paper.

The remaining sections of this paper are as follows: Section II describes the PDE model. Section III illustrates the application of PDE on the IEEE 34 test node feeder along with data generation via Monte Carlo simulation. Section IV presents PDE results with synthetic demand and EV data for the IEEE 34 test node feeder. Finally, Section V encapsulates the findings and conclusions.

This work was supported in part by the US National Science Foundation Grants: CNS #2318612 and ECCS #2234032.

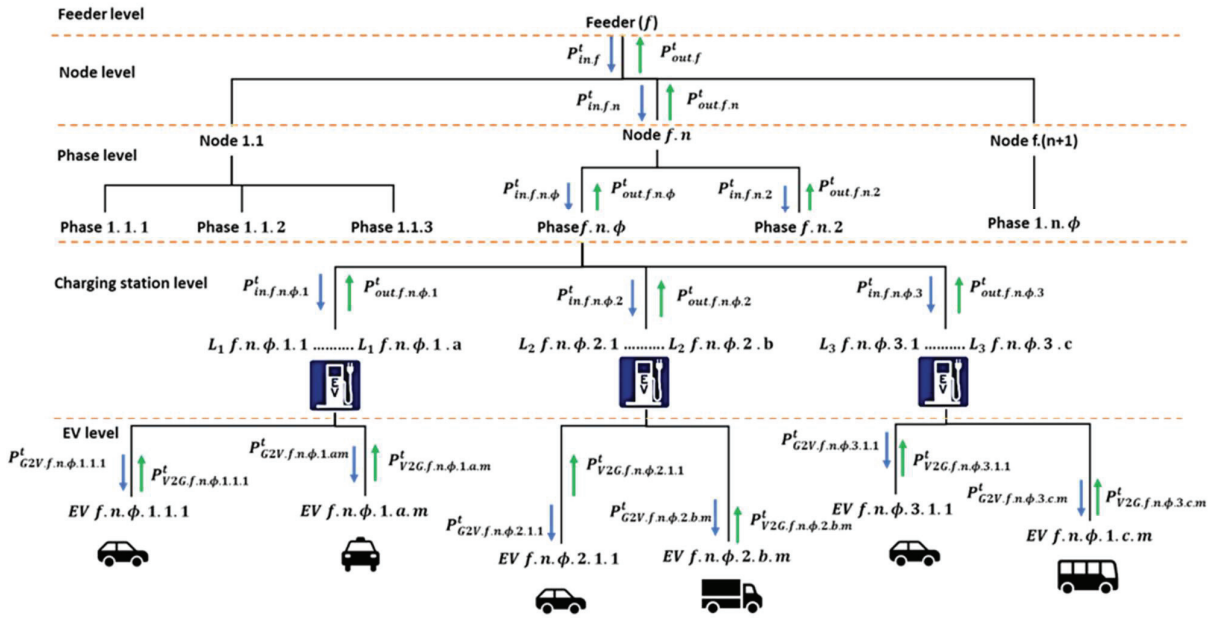

Fig. 1. Hierarchical diagram of depitcing the Feeder level, Node level, Phase level and EV level in a distribution system.

II. Power Dispatch Estimation

Power dispatch estimation harnessing V2G technology in any distribution system [10] involves two steps, namely: a) allocation of EVGIs for the nodes and b) EV data generation. In the proposed PDE model, the following foundational assumptions are made:

- Discharging levels are functionally analogous to charging levels with bidirectional inverter capabilities.
- Discharge rate is within the safe envelope for the batteries as in the case of charging. Furthermore, degradation in battery efficiency is neglected in these studies.
- Allocation of the distribution system infrastructure maximizes G2V while enabling V2G.
- Price per discharging kWh is same across the distribution system.

The EVGI allocation [11], PDE formulation and EV data generation in a distribution system are described in Sections II.A, II.B and II.C, respectively.

A. Allocation of EVGIs

Based on the aforementioned assumptions, the EVGI allocation is carried out with the goal of minimizing charging times within the constraints of the distribution system. The grid infrastructure supports bidirectional power flow, enabling both charging and discharging. Priority for EVGI allocation is first given to L_3 chargers followed by L_2 chargers and then L_1 chargers. The allocation of EVGI is determined solely by the rated power of the node.. L_1 and L_2 stations are designed to support bidirectional power flow, encompassing both V2G and G2V capabilities. In contrast, L_3 stations are presumed to only support G2V at their specified ratings due to EV battery safety considerations, and L_3 stations are assumed to discharge at the L_2 rate. Therefore, L_1 and L_2 stations operate either as G2V or V2G, allowing unoccupied G2V stations to facilitate V2G operations. The power levels for charging and discharging are set at 1 kW and 19 kW for L_1 and L_2, respectively, while L_3 stations charge at 50 kW and discharge at 19 kW as specified in references [12-15].

B. Formulation of PDE

The V2G PDE is formulated based on the system infrastructure, which includes factors such as the number of phases, nodes, and several types of charging levels. The estimated network V2G power transaction is described by (1(a)), where ϕ represents the phase (1, 2, 3), n denotes the feeder node number, m represents the EV number and *a, b, c* indicates the number of charging station levels L_j, where j = 1, 2, 3 respectively, for the node at a given time instant, t. L_1 and L_2 are types of AC charging and L_3 can accommodate the DC fast charging (DCFC) and extreme fast charging (XFC). Therefore, the number of L_3 stations, c is divided into two namely CDCFC and CXFC representing number of DCFCs and XFCs. Total V2G power in the network, $P_{V2G}(t)$ is illustrated by (1a).

$$P_{f,V2G}(t) = \sum_{n=1}^{N}\sum_{\phi=1}^{3}(P_{n,\phi,L_1}(t) + P_{n,\phi,L_2}(t) + P_{n,\phi,L_3}(t)) \quad (1a)$$

$$P_{n,\phi,L_1}(t) = \sum_{i=1}^{a} P_{L_1,m}(t) \quad (1b)$$

$$P_{n,\phi,L_2}(t) = \sum_{i=1}^{b} P_{L_2,m}(t) \quad (1c)$$

$$P_{n,\phi,L_{3,DCFC}}(t) = \sum_{j=1}^{c_{DCFC}} P_{L_{3,DCFC},m}(t) \quad (1d)$$

$$P_{n,\phi,L_{3,XFC}}(t) = \sum_{j=1}^{c_{XFC}} P_{L_{3,XFC},m}(t) \quad (1e)$$

To ensure system security of the distribution system, the maximum power supplied for a phase must not be surpassed and the node voltages maintained within their limits. In this study, the maximum V2G discharging power per phase in the network is considered fixed, and the system node voltages are assumed to operate within a range of 1.00 ± 5% p.u. The maximum V2G power per phase can be represented by (2).

$$P_{n,\phi,max} = a.P_{L_1,max} + b.P_{L_2,max} + c.P_{L_3,max} \quad (2)$$

The estimated V2G dispatch for the network will depend on the maximum dischargeable hosting capacity per phase in the network as described by (2). The V2G estimation for a given node, *n,* within the system is given by (3), where the total V2G power supplied at time t is denoted by $P_{n,V2G}(t)$, the

load at time t is represented by $D_n(t)$, the EV charging demand by $P_{n,G2V}(t)$, the surplus power outflow is denoted as $P_{n,out}(t)$ and the power intake from the grid as $P_{n,in}(t)$.

$$P_{n,V2G}(t) = D_n(t) + P_{n,G2V}(t) + P_{n,out}(t) - P_{n,in}(t) \quad (3)$$

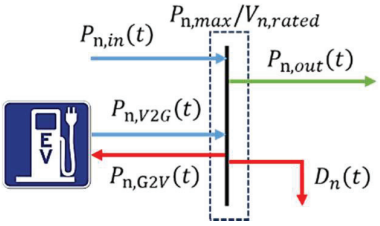

Fig. 2. Nodal power flows in a distribution with an EVGI and other loads.

As described in (3), an effective method of V2G demand estimation will boost the power dispatch resulting the reduction of the $P_{n,in}(t)$ which allows for peak power reduction. Therefore, the voltage stability will be ensured. Fig. 2 offers a general visualization of the nodal power inflows and outflows corresponding to these scenarios where the $P_{n,max}$ is the maximum power rating in kW and $V_{n,rated}$ is the rated voltage in kV of the n^{th} node, respectively. Fig. 1 describes the hierarchical diagram for the connected V2G infrastructure in a feeder, f, of a distribution network. V2G PDE, $P_{m,Lj,n,V2G}(t)$, for a certain charging level L_j, at the node n can be formulated by (4), (5a) and (5b), for the m^{th} EV, where the BC is the battery capacity of the vehicle at a certain level.

$$P_{L_j,\phi,n,V2G}(t) = \sum_{m=1}^{N_{PHEV}} \frac{E_m(t)}{T_m} + \sum_{m=1}^{N_{BEV}} \frac{E_m(t)}{T_m} + \sum_{m=1}^{N_{FCEV}} \frac{E_m(t)}{T_m} \quad (4)$$

$$P_{m,L_j,n,V2G}(t) = \frac{E_m(t)}{T_m} \quad (5a)$$

$$P_{m,L_j,n,V2G}(t) = \frac{(SOC_{start,m} - SOC_{stop,m}) \times BC_m}{T_{stop,m} - T_{start,m}} \quad (5b)$$

C. EV Data Generation

For the V2G estimation of the power dispatch, numerous factors are considered within the proposed model, as described below.

1) *Available number of EVs, $N_{n,Lj,EV}(t)$*:
$$N_{n,L_j,EV}(t) = N_{n,L_j,PHEV}(t) + N_{n,L_j,BEV}(t) + N_{n,L_j,FCEV}(t) \quad (6)$$
where, $N_{n,Lj,BEV}(t)$ is the number of battery EVs, $N_{n,Lj,PHEV}(t)$ is the number of PHEVs and the $N_{n,Lj,FCEV}(t)$ the number of fuel cell EVs at the charging station of level L_j.

2) *Available time duration, T_m*:
$$T_{m,min} \le T_m \le T_{m,max} \quad (7)$$
where $T_{m,min}$ is the minimum available time, $T_{m,max}$ is the maximum available time for the m^{th} EV at node n, charging level L_j.

3) *Available capacity, $E_m(t)$*:
$$E_m(t) \le E_{m,start}(t) - E_{m,stop}(t) \quad (8)$$
where the $E_{m,stop}(t)$ and the $E_{m,start}(t)$ are the available battery capacities of the m^{th} EV at the end and the start of the discharging at node n, charging level L_j, determined by the State of Charge (SOC). For the scope of this paper, the battery's life-time is assumed to be within the safe envelope at each discharging cycle with the lower limit of $E_{m,stop}(t)$. In other words, no battery performance degradation. However, with battery degradation over time, a battery degradation factor will account for losses during G2V and V2G.

4) *Location of the EV*
In terms of the SOC the location of the EV is taken into consideration for the maximum possible discharge for the nearest available node.

5) *Availability of the discharging node*
Even if a certain EV is available at a specific location, the closest charging station should be available for the discharge.

6) *Discharging power levels*
$$P_{V2G,m}(t) \le min\{P_{BV2G,m}\} \quad (9)$$
Here, $P_{V2G,m}$ denotes the dispatched power, and $P_{BV2G,m}$ represents the constraint imposed by the battery corresponding to a specific SOC in the m^{th} EV.

First, the $N_{n,Lj,EV}(t)$ is generated assuming the domestic loads (DOM) can only support L_1 and L_2 EVGI levels, with a maximum of two EVs per node. The nodes for industrial (IND) and commercial (COM) loads are assumed to be occupied for 18 hours per day at L_2 EVGIs, with a 3-hour period for V2G transactions per EV, allowing for six EVs per EVGI. L_1 EVGIs in the IND and COM nodes are assumed to be occupied for 20 hours per day, with a 4-hour period for V2G per EV, accommodating five EVs per EVGI. L_3 EVGIs are assumed to accommodate six EVs per station in each distribution system. Then the EV data for T_m, E_m, and the $SOCs$ were generated using the Monte Carlo algorithm.

III. Modified IEEE 34 Test System

The test system for this study is the IEEE 34 test node feeder illustrated in Fig. 3, representing an actual feeder in Arizona [16-18]. The configuration details of the IEEE 34 test node feeder can be found in [16] with overhead line configurations, line segment data, transformer data, load data, spot loads, distributed loads, shunt capacitors, regulator data, impedances, power flow results, voltage profiles and power flow data.

A. Generation of Dynamic Load Profiles

The 34 test nodes are categorized into three types of loads, namely: DOM, IND and COM. The demand curves of the selected nodes for the estimation during a weekday and weekend day, according to the data presented in [19] and the decision tree (DT) approach proposed in [11], are depicted in Fig. 4. Table A.I presents the categorization of loads, IND in dark orange, COM loads in light orange and DOM loads in mild orange.

B. Allocation of EVGIs in the IEEE 34 Test Node Feeder

According to Section II. A, and the DT proposed in [11], the EVGIs are allocated for the test node feeder with the dynamic load profiles. It is assumed that DOM load nodes can only support L_1 and L_2 EVGI stations with a maximum of two to three EVs, whereas COM and IND load nodes can support all charging levels. The EVGI allocation is shown in Table A.I and the IEEE 34 test node system with EVGIs allocated is depicted in Fig. 3. The predefined load parameters from [16] are taken as the load constraints for the modified IEEE 34 test node feeder.

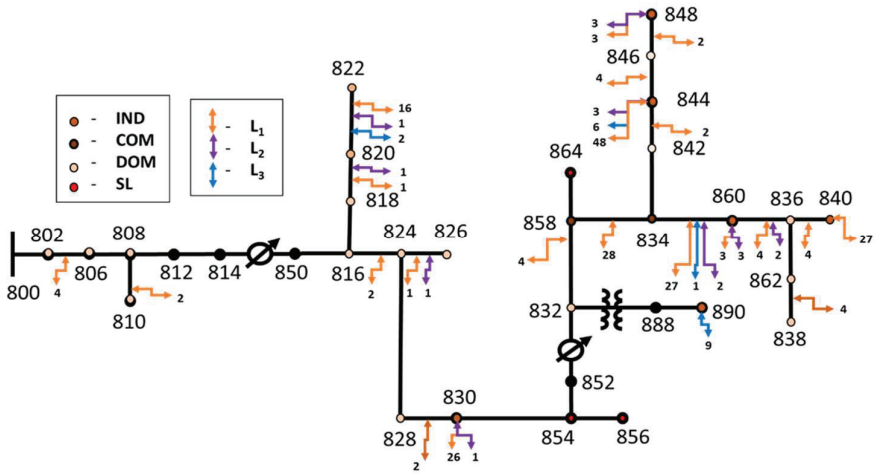

Fig. 3. IEEE 34 test node feeder with allocated EVGI [11].

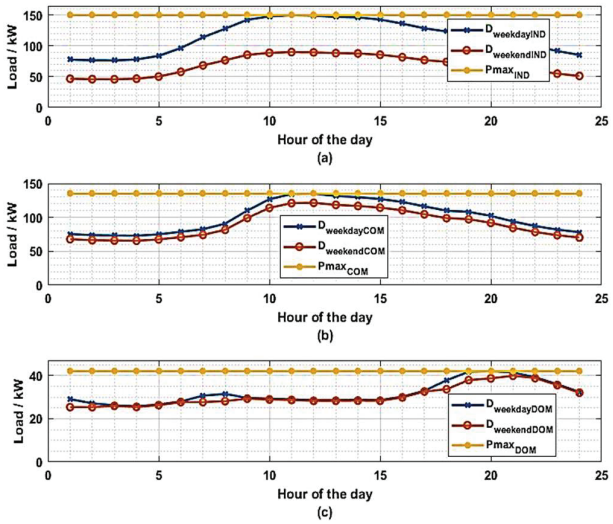

Fig. 4. (a) Daily load curves of IND 890,1 for weekday and weekend; (b) Daily load curve of COM 820-822,1 for weekday and weekend; (c) Daily load curve of DOM 860-836,1 for weekday and weekend.

C. EV Data Generation for IEEE 34 Test Node Feeder

For this study, the data for EV availability has been generated over a period of 24 hours based on several factors as mentioned in Section II.C. The Monte Carlo algorithm has been used to generate data.

1) Available number of EVs

Initially, the available number of EVs has been ascertained in relation to the total number of allocated EVGIs [11]. The system encompasses a total of 247 EVGIs, accommodating various charging/discharging levels including L_1, L_2, and L_3. Assuming each DOM unit hosts only two EVs, there are a collective 76 EVs within DOMs, distributed as 68 at L_1 level and eight at L_2 level. For IND and COM settings, EVGIs are presumed to operate for 18 hours daily, facilitating an average discharge duration of 3 hours per L_2 EV and a 20-hour daily utilization period with a 4-hour average discharge period for V2G discharge at L_1 level. Moreover, L_3 charging is anticipated to serve six EVs per day per EVGI.

2) Available time duration of EV

Each EV is available in the above section *1)* which drops under IND, COM, or DOM and the EVGI power levels of L_1, L_2, L_3, has a hypothetical availability profile throughout the 24 hours. Taking an average milage 240 for an EV and assuming the daily milage is about 70, a particular EV is charged every three days. The IND and COM loads are assumed to discharge no more than an hour.

3) Available capacity of EV

The available capacity is generated in terms of the SOC for each vehicle in an hourly manner over 24 hours. With the *BC* for the L_1, L_2, and L_3 discharging levels, the available capacity for the hour can be calculated. The *BCs* for L_1, L_2, and L_3 are taken in between 1/3 and 1/2 of the *BC*. The discharge rates are taken as 1, 19 and 19 kW for EVGIs in L_1, L_2, L_3, respectively, where the L_3 is discharging at the same rate as L_2 for the safety considerations of the batteries.

4) Location of the EV

Location will indicate how closer the EV is to an EVGI with respect to change in SOC (ΔSOC) when it reaches the EVGI. The available capacity E_m will vary according to ΔSOC. This factor is more critical for the COM and IND loads.

5) Availablility of the discharging node

The availability of a node is represented by the availability of the EVGI allocated to each node as shown in Appendix A.1. Each station connected in a node has a hypothetical availability profile over 24 hours according to its load type.

6) Discharging power levels

The power levels for the specified discharging levels are considered as 1 kW, 19 kW and 19kW for L_1, L_2, and L_3, respectively. L_3 is discharged at the same rate of L_2 for the safety aspects of the batteries [12-15].

IV. Results and Discussions

The allocation of EVGIs as reported in [11] for the IEEE 34 node test system is detailed in Table A.I. A total number of 247 EVGIs are allocated, namely: 132 for IND, comprising 107 L_1s, 10 L_2s, and 15 L_3s, 38 EVGIs for DOM consisting of 34 L_1s and 4 L_2s, and 77 EVGIs for COM consisting of 71 L_1s, 2 L_2s and 4 L_3s. For the EV generated data based on the

above decision variables, the daily $P_{n,V2G}(t)$ in kW is calculated using (4a), (4b) and (5). The estimated $P_{n,V2G}(t)$ is shown in Fig. 5 for a weekday and a weekend for sample nodes namely, IND 890,1, COM 820-822,1 and DOM 860-836,1. The V2G demand of IND and COM EVGIs is illustrated only for the L_2 and L_3. The data utilized for Fig.5 is shown in Table A.II-IV. As shown in Fig. 5 above for selected IND, COM, and DOM nodes, the estimated practical V2G demand is varying over the period of 24 hours. The maximum V2G is limited by the nodal ratings [16], for example, nodes IND 890,1, COM 820-822,1 and DOM 860-836,1 are limited to 150 kW, 135 kW and 42 kW, respectively. The practical possible maximum V2G discharge rate is based on the allocated EVGI type. The discharge rate of different EVGI types is described in Section II.A.

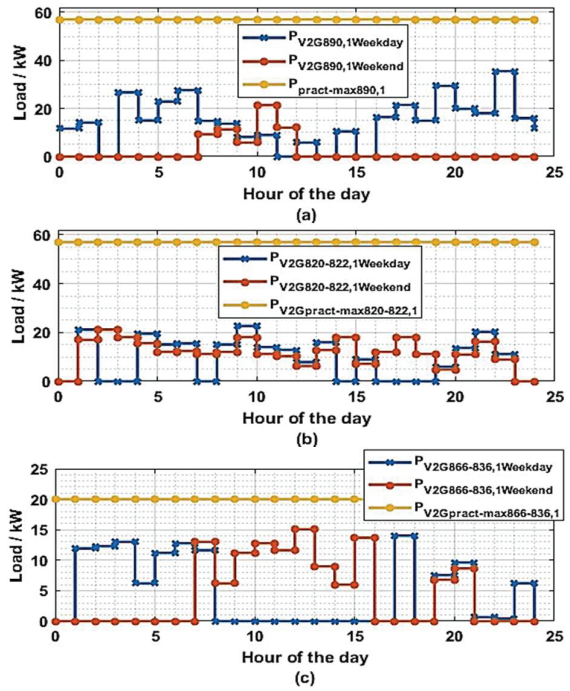

Fig. 5. (a) Estimated and practical V2G demand of IND 890,1; (b) Estimated and practical V2G demand of COM 820-822,1; (c) Estimated and practical V2G demand of DOM 860-836,1, blue line represents the estimated V2G demand in a weekday; orange line represents the estimated V2G demand in a weekend, yellow line represents the practical possible maximum V2G demand for the given IND, COM and DOM nodes.

V. Conclusion

The integration of electric vehicles into distribution systems presents both challenges and opportunities for optimal energy management and operations. This paper has presented the development of a power dispatch estimation model from EVs, based on the capabilities of a distribution system and the availability of EVs. By considering the spatiotemporal dependencies inherent in EV charging and discharging patterns, the PDE model proposed herein accounts for the distribution system structure with optimal EVGIs allocation. With typical PDE results illustrated on the IEEE 34 test node feeder distribution system, the potential of V2G power dispatch have been demonstrated. As the adoption of EVs continues to rise, the development and refinement of such PDE models will play a pivotal role in enhancing the efficiency and sustainability of our energy infrastructure with enhanced operation and management. Future work involves a dynamic simulation of the distribution system with the EVGIs and their G2V/V2G profiles to account for system voltage profiles and Volt-Var control.

References

[1] IEA, "Global EV Outlook 2023", IEA, Paris, 2023, https://www.iea.org/reports/global-ev-outlook-2023.

[2] BloombergNEF, "Electric Vehicle Outlook 2023", https://about.bnef.com/electric-vehicle-outlook.

[3] H. Kikusato, "Electric Vehicle Charge–Discharge Management for Utilization of Photovoltaic by Coordination Between Home and Grid Energy Management Systems," IEEE Transactions on Smart Grid, vol. 10, no. 3, pp. 3186-3197, May 2019, doi: 10.1109/TSG.2018.2820026.

[4] K. Clement-Nyns, E. Haesen, J. Driesen, "The impact of vehicle-to-grid on the distribution grid", Electric Power Systems Research, vol. 81, no. 1, pp. 185-192, 2011, ISSN 0378-7796, https://doi.org/10.1016/j.epsr.2010.08.007.

[5] S. Huang, W. Liu, J. Zhang, C. Liu, H. Sun, Q. Liao, "Vehicle-to-grid workplace discharging economics as a function of driving distance and type of electric vehicle", Sustainable Energy, Grids and Networks, vol. 31, 2022, 100779, ISSN 2352-4677, https://doi.org/10.1016/j.segan.2022.100779.

[6] Y. Ma, T. Houghton, A. Cruden and D. Infield, "Modeling the Benefits of Vehicle-to-Grid Technology to a Power System," in IEEE Transactions on Power Systems, vol. 27, no. 2, pp. 1012-1020, May 2012, doi: 10.1109/TPWRS.2011.2178043.

[7] A. Saber A, G. K. Venayagamoorthy, "Intelligent Unit Commitment with V2G - A Cost-Emission Optimization", Journal of Power Sources, vol. 195, February 2010, pp. 898-911

[8] P. Herath, G. K. Venayagamoorthy, "Scalable Residential Demand Response Management", IEEE Access, vol. 9, pp. 159133-159145, doi: 10.1109/ACCESS.2021.3119270, October 11, 2021

[9] T. K. Miao, V. K. Ramachandaramurthy, Y. J. Yong, "Integration of electric vehicles in smart grid: A review on vehicle to grid technologies and optimization techniques," Renewable and Sustainable Energy Reviews, Elsevier, vol. 53, pp. 720-732, 2016.

[10] W. H. Kersting, "Radial distribution test feeders," in IEEE Transactions on Power Systems, vol. 6, no. 3, pp. 975-985, Aug. 1991, doi: 10.1109/59.119237.

[11] I. K. Subasinghe, G. K. Venayagamoorthy, "A Methodology for Estimating Allocation of Electric Vehicle Grid Interfaces in a Distribution System" , IEEE Power Africa Conference 2024.

[12] S. Palanisamy, S. Chenniappan, S. Padmanaban, "Distribution System Planning," Fast-Charging Infrastructure for Electric and Hybrid Electric Vehicles: Methods for Large-Scale Penetration into Electric Distribution Networks, IEEE, 2023, pp. 59-81, doi: 10.1002/9781119987772.ch11.

[13] IEC 61851-1:2017(2017), "Electric vehicle conductive charging system- Part 1", General requirements. 12-15 IEC Standards.

[14] U. S. Department of Transportation."Charging Forward: Rural EV Toolkit Version 2", May 2023, online source: https://www.transportation.gov/rural/ev/toolkit/ev-basics/charging-speeds.

[15] P. Vishwas, R. Singh, "End-to-End Direct-Current-Based Extreme Fast Electric Vehicle Charging Infrastructure Using Lithium-Ion Battery Storage" Batteries 9, no. 3: 169, 2023, https://doi.org/10.3390/batteries9030169

[16] "Radial Test Feeders", IEEE Distribution System Analysis Subcommittee, online source: http://www.ewh.ieee.org/soc/pes/dsacom/testfeeders.html.

[17] N. Mwakabuta, A. Sekar, "Comparative Study of the IEEE 34 Node Test Feeder under Practical Simplifications," 2007 39th North American Power Symposium, Las Cruces, NM, 2007, pp. 484-491, doi: 10.1109/NAPS.2007.4402354.

[18] A. J. O. Owuor, J. L. Munda, A. A. Jimoh, "The IEEE 34 node radial test feeder as a simulation testbench for Distributed Generation," IEEE Africon '11, Victoria Falls, Zambia, 2011, pp. 1-6, doi: 10.1109/AFRCON.2011.6072095.

[19] Southern California Edison, 2023 Dynamic Load Profiles, online resource: https://www.sce.com/regulatory/load-profiles/dynamic-load-profiles.

VI. Appendix

TABLE A. I Allocated EVGIs And The Total Available EVs For The IEEE 34 Test Node Feeder

n.ϕ	Vrated (kV)	Pmax (kW)	L1			L2			L3			
			Available EVs	Num. of L1	C/D Rating (kW)	Available EVs	Num. of L2	C/D Rating (kW)	Available EVs	C Rating (kW)	Num. of L3	D Rating (kW)
860,1	24.9	20	-	-	1	6	1	19	-	50	-	19
860,2	24.9	20	-	-	1	6	1	19	-	50	-	19
860,3	24.9	20	-	-	1	6	1	19	-	50	-	19
840,1	24.9	9	45	9	1	-	-	19	-	50	-	19
840,2	24.9	9	45	9	1	-	-	19	-	50	-	19
840,3	24.9	9	45	9	1	-	-	19	-	50	-	19
844,1	24.9	135	80	16	1	6	1	19	12	50	2	19
844,2	24.9	135	80	16	1	6	1	19	12	50	2	19
844,3	24.9	135	80	16	1	6	1	19	12	50	2	19
848,1	24.9	20	5	1	1	6	1	19	-	50	-	19
848,2	24.9	20	5	1	1	6	1	19	-	50	-	19
848,3	24.9	20	5	1	1	6	1	19	-	50	-	19
890,1	4.16	150	-	-	1	-	-	19	18	50	3	19
890,2	4.16	150	-	-	1	-	-	19	18	50	3	19
890,3	4.16	150	-	-	1	-	-	19	18	50	3	19
830,1	24.9	10	50	10	1	-	-	19	-	50	-	19
830,2	24.9	10	50	10	1	-	-	19	-	50	-	19
830,3	24.9	25	30	6	1	6	1	19	-	50	-	19
820-822,1	24.9	135	80	16	1	6	1	19	12	50	2	19
858-834,2	24.9	15	75	15	1	-	-	19	-	50	-	19
858-834,3	24.9	13	65	13	1	-	-	19	-	50	-	19
834-860,1	24.9	16	80	16	1	-	-	19	-	50	-	19
834-860,2	24.9	20	5	1	1	6	1	19	-	50	-	19
834-860,3	24.9	110	50	10	1	-	-	19	12	50	2	19
802-806,2	24.9	30	2	2	1	-	-	19	-	50	-	19
802-806,3	24.9	25	2	2	1	-	-	19	-	50	-	19
808-810,2	24.9	16	2	2	1	-	-	19	-	50	-	19
818-820,1	24.9	34	2	1	1	-	1	19	-	50	-	19
816-824,2	24.9	5	2	2	1	-	-	19	-	50	-	19
824-826,2	24.9	40	2	1	1	-	1	19	-	50	-	19
828-830,1	24.9	7	2	2	1	-	-	19	-	50	-	19
832-858,1	24.9	7	2	2	1	-	-	19	-	50	-	19
832-858,3	24.9	6	2	2	1	-	-	19	-	50	-	19
860-836,1	24.9	30	2	1	1	-	1	19	-	50	-	19
860-836,2	24.9	10	2	2	1	-	-	19	-	50	-	19
860-836,3	24.9	42	2	1	1	-	1	19	-	50	-	19
836-840,1	24.9	18	2	2	1	-	-	19	-	50	-	19
836-840,2	24.9	22	2	2	1	-	-	19	-	50	-	19
862-838,2	24.9	28	2	2	1	-	-	19	-	50	-	19
842-844,1	24.9	9	2	2	1	-	-	19	-	50	-	19
844-846,2	24.9	25	2	2	1	-	-	19	-	50	-	19
844-846,3	24.9	20	2	2	1	-	-	19	-	50	-	19
846-848,2	24.9	23	2	2	1	-	-	19	-	50	-	19

TABLE A. II Data Generated For The Weekday Of IND 890,1

Hour of the day	SOCstart - ΔSOC - SOCend			Node availability			$P_{L3,1,V2G}$			$P_{890,1,V2G}$
	$DSOC_{L3,1}$	$DSOC_{L3,2}$	$DSOC_{L3,3}$	$L_{3,1,890,1}$	$L_{3,1,890,2}$	$L_{3,1,890,3}$	$P_{L3,1,V2G,1}$	$P_{L3,1,V2G,2}$	$P_{L3,1,V2G,3}$	
1	0.32	0.38	0.42	1	0	1	6.17	0.00	7.96	14.13
2	0.74	0.30	0.70	0	0	0	0.00	0.00	0.00	0.00
3	0.73	0.42	0.25	1	1	1	13.87	8.06	4.77	26.69
4	0.47	0.47	0.32	1	0	1	8.91	0.00	6.09	15.01
5	0.79	0.42	0.44	1	1	0	14.95	7.92	0.00	22.87
6	0.78	0.68	0.68	1	0	1	14.77	0.00	12.85	27.62
7	0.79	0.41	0.37	0	1	1	0.00	7.85	7.01	14.85
8	0.38	0.52	0.72	0	0	1	0.00	0.00	13.66	13.66
9	0.30	0.43	0.74	0	1	0	0.00	8.16	0.00	8.16
10	0.42	0.47	0.44	0	1	0	0.00	8.99	0.00	8.99
11	0.47	0.75	0.75	0	0	0	0.00	0.00	0.00	0.00
12	0.42	0.31	0.32	0	1	0	0.00	5.82	0.00	5.82
13	0.68	0.37	0.65	0	0	0	0.00	0.00	0.00	0.00
14	0.41	0.49	0.55	0	0	1	0.00	0.00	10.47	10.47
15	0.43	0.72	0.58	0	0	0	0.00	0.00	0.00	0.00
16	0.38	0.41	0.49	1	0	1	7.16	0.00	9.25	16.41
17	0.64	0.77	0.36	0	1	1	0.00	14.58	6.88	21.46
18	0.37	0.78	0.32	0	1	0	0.00	14.91	0.00	14.91
19	0.48	0.49	0.57	1	1	1	9.18	9.26	10.92	29.36
20	0.39	0.79	0.66	1	0	1	7.32	0.00	12.52	19.84
21	0.42	0.36	0.59	0	1	1	0.00	6.86	11.18	18.04
22	0.70	0.68	0.49	1	1	1	13.31	12.93	9.27	35.51
23	0.25	0.59	0.73	1	1	0	4.77	11.20	0.00	15.97
24	0.32	0.61	0.55	0	1	0	0.00	11.60	0.00	11.60

TABLE A. III Data Generated For The Weekday Of COM 820-822,1

Hour of the day	SOCstart - ΔSOC - SOCend			Node availability			$P_{820-822,1,V2G}$			$P_{820-822,1,V2G}$
	$DSOC_{L2,1}$	$DSOC_{L3,1}$	$DSOC_{L3,2}$	$L_{2,1,820-822,1}$	$L_{3,1,820-822,1}$	$L_{3,1,820-822,2}$	$P_{L2,1,V2G,1}$	$P_{L3,1,V2G,1}$	$P_{L3,1,V2G,2}$	
1	0.39	0.73	0.29	1	1	1	7.32	13.87	5.47	21.19
2	0.42	0.47	0.54	0	0	1	0.00	0.00	10.25	0.00
3	0.70	0.79	0.28	0	0	1	0.00	0.00	5.29	0.00
4	0.25	0.78	0.69	1	1	1	4.77	14.77	13.07	19.54
5	0.32	0.79	0.69	0	1	1	0.00	15.09	13.05	15.09
6	0.44	0.38	0.44	1	1	1	8.33	7.20	8.30	15.53
7	0.68	0.30	0.75	0	0	1	0.00	0.00	14.22	0.00
8	0.37	0.42	0.75	1	1	0	7.01	8.06	0.00	15.06
9	0.72	0.47	0.74	1	1	1	13.66	8.99	14.11	22.65
10	0.74	0.42	0.34	1	0	0	14.02	0.00	0.00	14.02
11	0.44	0.68	0.25	0	1	1	0.00	12.88	4.79	12.88
12	0.75	0.41	0.38	0	1	1	0.00	7.85	7.21	7.85
13	0.32	0.52	0.43	1	1	0	6.05	9.96	0.00	16.01
14	0.65	0.43	0.38	0	0	0	0.00	0.00	0.00	0.00
15	0.55	0.47	0.64	0	1	0	0.00	8.99	0.00	8.99
16	0.58	0.75	0.37	0	0	0	0.00	0.00	0.00	0.00
17	0.49	0.31	0.48	0	0	1	0.00	0.00	9.18	0.00
18	0.36	0.37	0.39	0	0	0	0.00	0.00	0.00	0.00
19	0.32	0.49	0.42	1	0	1	5.99	0.00	7.96	5.99
20	0.57	0.72	0.70	0	1	1	0.00	13.69	13.31	13.69
21	0.66	0.41	0.25	1	1	0	12.52	7.73	0.00	20.25
22	0.59	0.77	0.32	1	0	0	11.18	0.00	0.00	11.18
23	0.49	0.78	0.44	0	0	1	0.00	0.00	8.33	0.00
24	0.73	0.49	0.68	0	0	0	0.00	0.00	0.00	0.00

TABLE A. IV Data Generated For The Weekday Of DOM 860-836,3

Hour of the day	SOCstart - ΔSOC - SOCend		Node availability		$P_{860-836,3,V2G}$		$P_{860-836,3,V2G}$
	$DSOC_{L1,1}$	$DSOC_{L2,2}$	$L_{1,3,860-836,1}$	$L_{2,3,860-836,1}$	$P_{L1,3,V2G,1}$	$P_{L2,3,V2G,1}$	
1	0.65	0.59	1	1	0.65	11.27	11.92
2	0.70	0.65	0	1	0.00	12.30	12.30
3	0.73	0.68	0	1	0.00	13.00	13.00
4	0.36	0.31	1	1	0.36	5.83	6.19
5	0.63	0.59	0	1	0.00	11.21	11.21
6	0.68	0.64	1	1	0.68	12.12	12.79
7	0.65	0.61	0	1	0.00	11.63	11.63
8	0.60	0.57	0	0	0.00	0.00	0.00
9	0.32	0.26	0	0	0.00	0.00	0.00
10	0.40	0.35	0	0	0.00	0.00	0.00
11	0.47	0.43	0	0	0.00	0.00	0.00
12	0.62	0.58	0	0	0.00	0.00	0.00
13	0.41	0.35	0	0	0.00	0.00	0.00
14	0.34	0.30	0	0	0.00	0.00	0.00
15	0.79	0.75	0	0	0.00	0.00	0.00
16	0.40	0.35	0	0	0.00	0.00	0.00
17	0.79	0.74	0	1	0.00	14.03	14.03
18	0.61	0.55	0	0	0.00	0.00	0.00
19	0.42	0.38	1	1	0.42	7.13	7.56
20	0.56	0.51	0	1	0.00	9.62	9.62
21	0.66	0.61	1	0	0.66	0.00	0.66
22	0.43	0.39	1	0	0.43	0.00	0.43
23	0.36	0.33	0	1	0.00	6.22	6.22
24	0.57	0.53	0	0	0.00	0.00	0.00